Journal of the Serbian Society for Computational Mechanics / Vol. 18 / No. 1, 2024 / pp 45-66 / original paper
(10.24874/jsscm.2024.18.01.04)

MODELLING OF DAMAGE IN COMPOSITES USING SMOOTH PARTICLE HYDRODYNAMICS METHOD

Rade Vignjević[1*] [0000-0002-4677-068X], Tom De-Vuyst[2] [0000-0002-4372-4055] and Nenad Đorđević[1*] [0000-0002-2729-5721]

[1] Department of Mechanical and Aerospace Engineering, Centre for Assessment of Structures and Materials under Extreme Conditions, Brunel University London, Cambridge CB21 6AL, UK
e-mail: nenad.djordjevic@brunel.ac.uk
[2] University of Hertfordshire, Hatfield, Hertfordshire, AL10 9AB, UK
**corresponding author*

Abstract

This paper aims at the development and implementation of an algorithm for the treatment of damage and fracture in smooth particle hydrodynamic (SPH) method, where free surface, crack opening, including its propagation and branching is modelled by weakening the interparticle interactions combined with the visibility criterion. The model is consistent with classical continuum damage mechanics approach, but does not use an effective stress concept. It is a difficult task to model fracture leading to fragmentation in materials subjected to high-strain rates using continuum mechanics. Meshless methods such as SPH are well suited to be applied to fracture mechanics problems, since they are not prone to the problems associated with mesh tangling. The SPH momentum equation can be rearranged and expressed in terms of a particle-particle interaction area. Damage acts to reduce this area, which is ultimately set to zero, indicating material fracture. The first implementation of the model makes use of Cochran-Banner damage parameter evolution and incorporates a multiple bond break criterion for each neighbourhood of particles. This model implementation was verified in simulation of the one-dimensional and three-dimensional flyer plate impact tests, where the results were compared to experimental data. The test showed that the model can recreate the phenomena associated with uniaxial spall to a high degree of accuracy. The model was then applied to orthotropic material formulation, combined with the failure modes typical for composites, and used for simulation of the hard projectile impact on composite target.

Keywords: Smooth particle hydrodynamics (SPH), damage modelling, plate impact test, high velocity impact.

1. Introduction

A large portion of damage evolution and crack-growth research has been conducted with the use of mesh based numerical methods such as the finite element method, where two main types of crack representation model have been adopted: inter-element separation models and arbitrary crack-path models. In an inter-element separation model cracks are developed along element

boundaries, along the element edges (Xu and Needleman, 1994). The approach overestimates the fracture energy when the crack-paths are not in line with the element edges and the solution is often dependant on a well refined mesh (Rabczuk and Belytschko, 2004). This mesh requirement in the vicinity of crack path assumes that one can anticipate the failure mechanism of the material. This problem can be circumvented by the use of remeshing techniques (Belytschko and Black, 1999; Pandolfi et al. 1999; Ortiz and Pandolfi, 1999; Zhou and Molinari, 2004), although these methods tend to be very computationally expensive especially in the case of dynamic crack growth, where the amount of remeshing required is often substantial.

Arbitrary crack path models are more realistic in their approach to dealing with fracture but prove to be quite complicated within a mesh-based framework. One such example is the extended finite element method (Moës et al. 1999). Crack problems have been modelled in two and three dimensions (Stolarska et al. 2001; Moës et al. 2002; Gravouil et al. 2002) by coupling the technique with a level set method (Stolarska et al. 2001), i.e. modelling the 'crack-geometry' separately from the model. For fatigue-crack growth problems, discontinuities can be modelled quite accurately using this approach; however, a new level-set needs to be introduced for each individual crack, which would become very expensive for problems dealing with fragmentation. A remeshing approach has been adopted in Pandolfi et al. (1999) to extend the method to encompass crack branching.

'Meshless' methods, such as Smoothed Particle Hydrodynamics (SPH), do not require the use of a fixed spatial grid to provide connectivity between nodes. This eliminates the issues of mesh entanglement under large deformations, and allows for damage crack growth in an arbitrary direction, reducing the influence of the spatial discretisation on the solution. This also makes the meshless methods particularly suited to the application of fracture mechanics.

Extensive work has been conducted using the Element Free Galerkin (EFG) method, for several different failure modes. Single discontinuities have been modelled in 2D (Belytschko and Tabbara 1996) and 3D (Krysl and Belytschko, 1999) and a method that makes use of level sets to describe multiple cracks was proposed in Ventura et al. (2002). An interesting approach to dealing with multiple fractures called EFG-P was given in Rabczuk and Belytschko (2004) and Rabczuk and Belytschko (2007) for 2D and 3D respectively. The approach is developed as a particle method within the EFG framework, where the cracks are represented by introducing discontinuities at individual particles. A continuous crack then consists of a set of contiguous cracked particles.

From the literature it is clear that the technique adapted to model fracture is dependent on the exact failure mode that is being modelled. Cracks that develop slowly, such as those found in fatigue crack problems, are more suited to a global 'crack-geometry' approach, whilst the problems with multiple cracks lend themselves to a more 'local' description of damage.

This paper describes development of a damage model, based on an alternative approach to incorporate damage effects through the definition of particle-particle interaction area. The model is consistent with classical continuum damage mechanics approach, but unlike most of other models, it does not require the use of an effective stress. The model is intended to be able to initiate damage via an existing damage model, propagate the damage to the surrounding neighbourhood in accordance with a growth criterion and allow for bifurcation of cracks which will lead to fragmentation. The model was implemented in the in-house developed SPH code (Vignjevic et al. 2006; Vignjevic et al. 2009; Vignjevic et al. 2021) and validated against a number of tests cases, including the uniaxial plate impact tests, which there was available experimental data for and hard projectile impact on composite target.

The paper consists of six sections. Following the Introduction, an outline of the SPH method is provided in Section 2, with the novel approach for modelling damage described in Section 3.

The model implementation is subject of Section 4 and the Numerical examples for four test cases are given in Section 5. Section 6 outlines the conclusions and suggestions for future work.

2. Smooth Particle Hydrodynamics (SPH) method

In the SPH method, continuum is represented by a discrete set of particles that are assigned material properties and move according to the conservation laws. The method was originally developed for problems in astrophysics (Gingold and Monaghan 1977; Lucy 1977) and was updated to include solid mechanics problems by Libersky (1991). To date, the method has been applied to a wide spectrum of applications including hyper-velocity impact problems since Libersky et al. (1993).

A set of equations that are solved in an SPH code are the conservation laws written for a particle as follows:

Conservation of mass:

$$\frac{d\rho_i}{dt} = \rho_i \sum_j \frac{m_j}{\rho_j} \left[v_i - v_j \right] \nabla_i W_{ij} \tag{1}$$

Conservation of momentum:

$$\frac{dv_i}{dt} = -\sum_j m_j \left[\frac{\boldsymbol{\sigma}_i}{\rho_i^2} + \frac{\boldsymbol{\sigma}_j}{\rho_j^2} \right] \nabla_i W_{ij} \tag{2}$$

Conservation of energy:

$$\frac{de_i}{dt} = \frac{\boldsymbol{\sigma}_i}{\rho_i^2} \sum_j m_j \left[\mathbf{v}_i - \mathbf{v}_j \right] \nabla_i W_{ij} \tag{3}$$

Where summation is calculated over all neighbourhood particles j, m_j; is the mass of the j^{th} particle, $\boldsymbol{\sigma}$ is a Cauchy stress tensor, $\mathbf{v}_i$, $\mathbf{v}_j$ and, ρ_i, ρ_j are velocities and densities of corresponding particles; $\nabla_i W_{ij}$ is gradient of the SPH kernel function, taken with respect to the particle i.

The kernel function used in this paper to approximate the derivatives is the cubic spline kernel (Vignjevic et al 2009) defined as:

$$W\left(r,h\right) = \frac{b}{\pi h^a} \begin{cases} 1 - \frac{3}{2}q^2 + \frac{3}{4}q^3 & \text{if } 0 \le q \le 1 \\ \frac{1}{4}\left(2-q\right)^3 & \text{if } 1 \le q \le 2 \\ 0 & \text{otherwise} \end{cases} \tag{4}$$

where a is the number of spatial dimensions, b is a normalised constant which has the values; $2/3$, $10/7\pi$, $1/\pi$ in 1, 2 and 3 dimensions respectively; $q = r/h$, r is the position vector between a pair of particles and h is the finite range of the kernel, known as the SPH smoothing length.

There are several problems within the SPH method outlined in Swegle et al. (1994) such as the tensile instability, numerical fracture (Swegle et al. 1995) and zero energy modes (Vignjevic et al. 2000). The tensile instability is a numerical problem that manifests itself in the discretisation of the conservation equations, i.e. when the particles are under tensile stress their motion becomes unstable. The problem can be visualised as an unphysical clumping of the particles and, in some cases, leads to an early termination of the simulation. Analysis of the problem has determined that the instability depends on the sign of the product of the stress and the second derivative of the kernel function W'' (Swegle et al. 1995) which is mathematically expressed as:

$$W''\sigma > 0 \tag{5}$$

As long as the inequality (5) holds, the method is unconditionally unstable.

Severe manifestations of the tensile instability lead to another relevant problem for the basic SPH formulation known as a numerical fracture. Two SPH particles are considered to be neighbours if the distance between them is less than twice the smoothing length. Thus, all particles within a spherical domain are neighbours of the particle at the centre of that domain. This domain remains a sphere throughout the calculation, with either a fixed or variable radius. In the case of anisotropic deformation, two particles that should remain neighbours can move sufficiently far apart that they no longer influence each other. This results in a fracture that should not be present in the calculation.

The tension instability and numerical fracture can be eliminated completely by the use of a Lagrangian kernel function (Vignjevic et al. 2006; Vignjevic et al. 2021; Reveles 2007; Belytschko et al. 2000; Rabczuk et al. 2004). In the Total Lagrangian approach the initial state of the domain is regarded as the reference state. Consequently, the solutions of the conservation equations are expressed in terms of the material coordinates $\mathbf{X}$, instead of the spatial coordinates $\mathbf{x}$. The relation between these coordinates is given as follows:

$$\mathbf{x} = \phi\left(\mathbf{X}, t\right) \tag{6}$$

Where: ϕ is a mapping function and the initial conditions are usually defined for time $t = 0$ as:

$$\mathbf{x} = \phi\left(\mathbf{X}, 0\right) = \mathbf{X} \tag{7}$$

The deformation gradient is given as follows:

$$\mathbf{F} = \frac{\partial \mathbf{x}}{\partial \mathbf{X}} \tag{8}$$

and the conservation of mass is:

$$J_0 \rho_0 = J \rho \tag{9}$$

Where:

$$J = \det \mathbf{F} \tag{10}$$

All calculations are performed in the reference configuration and, therefore, the neighbourhood does not change. This method is valid for as long as the mapping between the domains exists. This cannot be achieved for the large shear deformations problems, which represent the limitation of this formulation.

3. Interaction area and damage variable

The concept of area vectors within the SPH method was introduced by Swegle (2000) in discussion of the tensile instability inherent in any basic SPH description. Motivated by the fundamental relationship between the stress tensor and a force exerted on a surface $\mathbf{P}$:

$$\mathbf{P} = \boldsymbol{\sigma} \cdot \mathbf{A} \tag{11}$$

the SPH momentum equation can be rewritten in terms of an interaction area between the particles. Starting from Newton's Second Law:

$$P_i = m_i a_i \tag{12}$$

one may rewrite equation (2) in the following form:

$$P_i = m_i a_i = -\sum_j m_i m_j \left[\frac{\boldsymbol{\sigma}_i}{\rho_i^2} + \frac{\boldsymbol{\sigma}_j}{\rho_j^2} \right] \nabla_i W_{ij} \tag{13}$$

By rearranging the equation above, the terms can be group to the form equivalent to equation (11):

$$P_i = -\sum_j A_{ij} \left[\left(\boldsymbol{\sigma}_i \right) \frac{\rho_j}{\rho_i} + \left(\boldsymbol{\sigma}_j \right) \frac{\rho_i}{\rho_j} \right] \tag{14}$$

$$A_{ij} = V_i V_j \nabla_i W_{ij} \tag{15}$$

where V_i is the volume of the i^{th} particle and A_{ij} is the interaction area vector, which determines the interaction between the particles i and j. The magnitude of the interaction area vector is equal to the area of the surface shown in Fig.1. and a direction of the vector is normal to the surface.

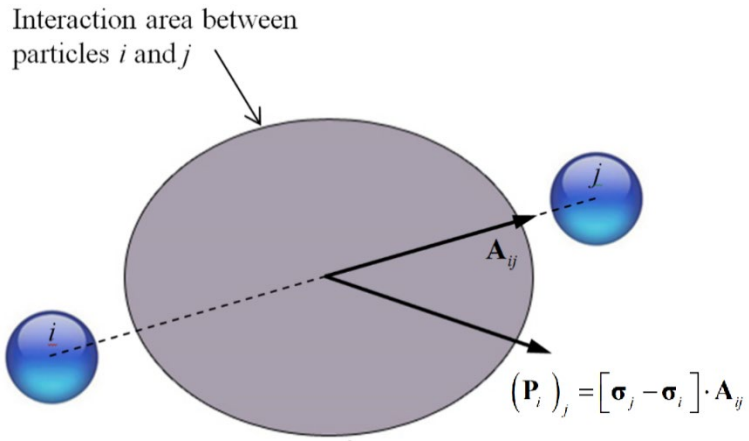

Fig. 1. Definition of particle – particle interaction area vector and the interaction force between the particles i and j

Equation (15) defines the interaction area vector in terms of the gradient of the kernel function as the area of stress action to produce a force between the particles.

Following the original work of Kachanov (1958), damage can be defined in terms of a scalar intrinsic damage variable ω, as a surface density of microcracks or microvoids within the material as:

$$\omega = \frac{\delta A_D}{\delta A} \tag{16}$$

Where δA and δA_D are, respectively, total area of a representative volume element (RVE) and area of microcracks and microvoids (damage). The effective area which carries out the load in a damaged material element is, then, the total area of damaged element, reduced for the area of damage, i.e. $\delta \tilde{A} = \delta A - \delta A_D$, which leads to the definition of the effective area in the damaged material as:

$$\delta \tilde{A} = \delta A\left(1-\omega\right) \tag{17}$$

In classical continuum mechanics, equation (17) was used for definition of an effective stress introduced by Kachanov (1958). However, the SPH method coupled with the concept of Swegle's interaction area offers an alternative approach to the common effective stress method of applying damage (Kachanov 1958; Lemaitre 1985). The interaction area A_{ij} can be thought of as being equivalent to the section area A defined in equation (11). Consequently, damage can be defined as an inter-particle variable ω_{ij} acting to reduce A_{ij} by directly applying the concept of continuum damage from equation (17). This definition does not require any modification of the stress tensor and equation (14) becomes:

$$P_i = -\sum_j \left[\left(\boldsymbol{\sigma}_i\right)\frac{\rho_j}{\rho_i} + \left(\boldsymbol{\sigma}_j\right)\frac{\rho_i}{\rho_j} \right] A_{ij}\left(1-\omega_{ij}\right) \tag{18}$$

Critical damage ($\omega_{ij} = 1.0$) assumes the material to have failed and the interaction area set to zero, causing the particles to cease being neighbours. To prevent unphysical interactions between fully damaged particles, once critical damage has been reached, all interpolated values are set to zero, by setting the gradient of the kernel function to zero, i.e. $\nabla_i W_{ij} = 0$.

In a standard Eulerian SPH code, a new neighbour search is competed at each time-step, implying a particle may gain or lose neighbours throughout the computation. This prevents the practical treatment of inter-particle damage, which is a material history variable and must be integrated in time. For this reason, we have chosen to use a Total Lagrangian description for the SPH interpolation i.e. the neighbourhood, where the particle-particle bonds are defined in the reference state and remain fixed throughout the computation. The interaction areas between particles can, therefore, be stored as material history variables and be updated with the damage variable at every time-step.

4. Model implementation

The model is implemented in the SPH research code (Vignjevic et al. 2009; Vignjevic et al. 2021). Any damage model can be used for the evolution of the damage variable ω_{ij} , as long as it represents a percentage of damaged material (i.e. micro-cracks/voids) for a particle-particle pair and is expressed in terms of local particle parameters. The failure criterion to initiate damage growth should also be dependent on inter-particle variables in order to correctly 'grow' a crack in the material. The method assumes that phenomena such as crack branching/bifurcation and crack joining are incorporated as a function of multiple bond failures in a localised region; and so careful selection of the failure criterion is required.

4.1 Calculation of inter-particle bond variables

For the calculation of the inter particle interaction/bond variables, it is necessary to calculate the traction between the particle pairs. Since SPH data are stored for the individual particles, the traction in the $(i \rightarrow j)$ direction, T_i and the $(i \leftarrow j)$ direction, T_j must first be obtained. From these tractions a composite value denoted as T_{ij} can be calculated for the traction between the particle pair. T_i and T_j are, therefore, the first components of the respective traction vectors in the direction of $(i \rightarrow j)$ and $(i \leftarrow j)$. These values can be obtained by rotating the full stress tensor to the new coordinate system for both particles in the pairs, but this is computationally expensive and will yield to the full stress tensors, whereas only the (1,1) values are required. Alternatively, one can obtain the traction vector $\hat{T}_i$ as the dot product of the unit vector denoted $\hat{n}_i$ and stress at the particle i , which projects the stress onto the $(i \rightarrow j)$ direction (Malvern 1969) as:

$$\hat{T}_i = \hat{n}_i \cdot \boldsymbol{\sigma}_i \tag{19}$$

Thus the direct stress at the i particle, in the $(i \to j)$ direction is simply the traction vector projected onto the $\hat{n}_i$. The traction between the particle pair, T_{ij} is then calculated as the average value of the traction in the individual particles:

$$T_{ij} = \frac{\left(T_i + T_j\right)}{2} \tag{20}$$

Von Mises stress for each particle-particle bond is simply the average of the Von Mises stress at both particles:

$$\overline{\sigma} = \frac{\overline{\sigma}_i + \overline{\sigma}_j}{2} \tag{21}$$

4.2 Damage and failure models

The model is currently implemented combined with Cochran-Banner model for modelling a spall in metals and modified Chang-Chang modelling for modelling impact on composites, as described in the following subsections.

4.2.1 Cochran-Banner

The modelling of spall failure is relevant for impact problems. An established damage model for this type of material failure is Cochran-Banner model (1977), which is used for damage evolution in the current model implementation, whist the damage initiated is controlled by a critical direct stress between particles. Damage initiation occurs when the direct stress T_{ij} between a pair of particles i and j, defined in equation (20), exceeds a user defined spall criterion Σ. After this point damage will begin to grow for that ($i - j$) pair. The Cochran-Banner damage growth model (Kachanov 1958) accounts for all positive changes in volume loaded above the material spall strength, including micro-crack and void growth:

$$\omega\left(x,t\right) = \int_0^t dV/A \quad \text{for} \quad dV > 0 \tag{22}$$

A three-dimensional version of this model is given in Mirkovic (2004) and it is this version that has been adapted for use with the interaction area outlined in the previous section.

The current change in volume for a particle may be calculated from the strain rate and the current time-step. More specifically, the change in volume for the area between the particles pair under consideration is defined as a mean value of the change in volume for the two particles:

$$dV_{ij} = \frac{dt}{2}\left[V_i \sum_{n=1}^{3} \dot{\varepsilon}_{i_n}^{pl} + V_j \sum_{n=1}^{3} \dot{\varepsilon}_{j_n}^{pl}\right] \tag{23}$$

where $\dot{\varepsilon}^{pl}$ is the effective plastic strain-rate. The cross-sectional area which the damage applies to is taken to be the magnitude of the interaction area A_{ij}, given in equation (15), so the Cochran-Banner damage parameter is simply:

$$\omega_{CB} = \frac{\int dV_{ij}}{\left|A_{ij}\right|} \tag{24}$$

The sign of dV_{ij} will depend on whether the force between the particles is compressive or tensile and the damage evolves only for a positive change in volume, i.e. void growth. It is clear that in a real continuum, compressive forces act to close the voids and the material can therefore regain some strength, but subsequent void re-growth under tension would be more rapid. However, current model implementation keeps the damage parameter constant for the time increments when the dV_{ij} is negative.

The inter-particle damage variable is updated using the following equation:

$$\omega_{ij_n} = \omega_{ij_{(n-1)}} + \left(\frac{\omega_{CB}}{\omega_{crit}}\right)^{2/3} \tag{25}$$

where ω_{crit} represents material parameter for critical damage. Total failure of the material is reached when $\omega_{ij} = 1.0$, so that the total damage of the material at time t is calculated as:

$$\omega_{ij} = \mathrm{MIN}\left[\omega_{ij}, 1.0\right] \tag{26}$$

In a real solid, localised damage would have an influence on the surrounding material, i.e. the damage of the model on a global scale. In an attempt to capture this phenomenon, a multiple bond-break criterion has also been added to the damage model.

4.2.2 A failure model used for composite materials

For the failure types other than the spall, damage initiation can be defined in terms of either stress or strain-based parameters. The Von Mises stress is typically used for isotropic damage models for ductile materials, whist the individual stress components or principal stresses are used for brittle materials, including Chang-Chang and Hashin failure criteria for composite materials. In the current implementation, the Chang-Chang failure criteria are used as criteria for the onset of damage of the inter-particle bonds (Chang and Chang 1987a; 1987b). Three criteria given from equation (27) to (29) are used for modelling fibre failure, matrix failure and delamination, respectively. The failure starts when the expressions reach a value of one; below one the material remains undamaged.

$$f_{fibre} = \left(\frac{\sigma_{aa}}{X_t}\right)^2 + \frac{\sigma_{ab}^2 + \frac{3}{4}\alpha\sigma_{ab}^4}{\frac{S_c^2}{2G_{ab}} + \frac{3}{4}\alpha S_c^4} \leq 1.0 \tag{27}$$

$$f_{matrix} = \left(\frac{\sigma_{bb}}{Y_t}\right)^2 + \frac{\sigma_{ab}^2 + \frac{3}{4}\alpha\sigma_{ab}^4}{\frac{S_c^2}{2G_{ab}} + \frac{3}{4}\alpha S_c^4} \leq 1.0 \tag{28}$$

$$f_{delamination} = \left(\frac{\sigma_{cc}}{S_n}\right)^2 + \left(\frac{\sigma_{bc}}{S_{bc}}\right)^2 + \left(\frac{\sigma_{ca}}{S_{ca}}\right)^2 \leq 1.0 \tag{29}$$

When one of these failure criteria is met, inter-particle bonds of that particle are allowed to accumulate damage. The bonds that can accumulate damage are restricted to one side of the particle, leaving the other half of the bonds intact. This creates a damage area, and subsequent crack, in the direction perpendicular to the loading direction. This is illustrated in Fig. 2 for the case of fibre failure. The fibre direction is indicated by the blue lines, and the particles that can accumulate damage are shown in red. Although the Chang-Chang criteria are used in the current model implementation, the concept presented is completely general and any other criteria to evaluate the onset of damage and the damage growth model can be adopted with this modelling approach.

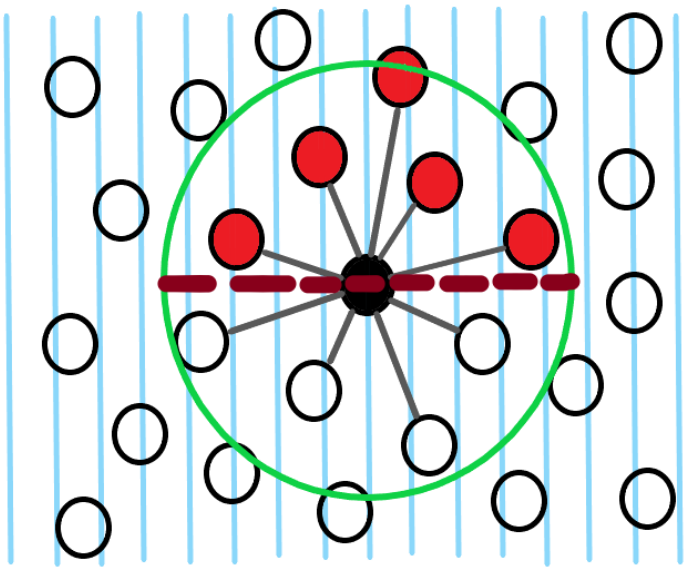

Fig. 2. Orthotropic damage formulation concept

5. Numerical examples

For the sake of numerical verification and validation and demonstration of the capability of the model based on the interactive area, a number of numerical test problems were run in our in-house developed SPH code (Vignjevic et al. 2006; 2009; 2021), including: flyer plate impact test with spall failure, tensile test of unidirectional composite based on ASTM3039 standard (2009) and hard projectile impact on flat composite plate. The simulation results are presented in the following subsections.

5.1 Flyer plate impact test with spall failure

The plate impact test used for validation is an experiment in which a 10 mm thick target plate was impacted by a 5 mm thick flyer plate at a velocity of 304 m/s, as illustrated in Fig. 3. Experimental data and material parameters for the plate impact test were obtained from Steinberg (1996). To record longitudinal stress data, a Manganin stress gauge was used on the rear surface of the target, supported with a 12 mm block of Polymethylmethacrylate (PMMA). The geometry of the flyer and the target were chosen so that the stress wave reflected from the free ends interact in the centre of the target plate, which is denoted as spall location in Fig. 3. This type of experiment is extremely useful for damage model validation purposes, since the experiment is designed to yield a uniaxial strain state inside the target plate.

The simulation of the experiment was conducted with an Elastic-Plastic-Hydrodynamic material model with a Grunaisen equation of state for the target and the PMMA. The one-dimensional model consisted of 540 particles: 100 in the flyer plate, 200 in the target plate and 240 in the PMMA. The SPH smoothing length was taken to be 1.3 times the initial inter-particle spacing. The spall strength for the target material was taken to be 1.2 GPa and the value of critical damage ω_{crit} , required for the Cochran-Banner damage model, was taken to be 0.007 .

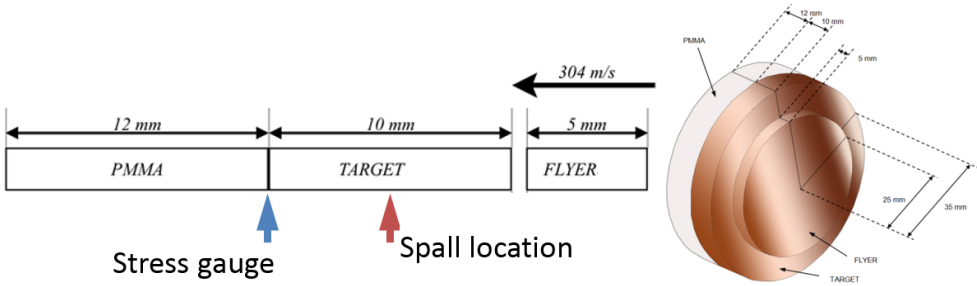

Fig. 3. Schematic representation of the plate impact: a cross section of a segment of the set up used for modelling (left) and 3D geometry (right)

In the plate impact test, the initially compressive waves generated at the contact between the flyer plate and target plan propagate through the material, reaching the free surfaces where they reflect as the tensile release waves. The tensile waves reflected from the back of the target plate and the back of the flyer plate then propagate through the material and superpose in the middle of the target plate causing high-tensile stress. When this tensile stress exceeds the spall strength of the material, the material fails, micro-voids form and coalesce in this region, ultimately leading to the generation of a new free surface. This free surface reduces the tensile stress in the material to zero and results in the reflection of the remainder of the release wave as a compressive wave. The same phenomena is expected in the simulations, since a new free surface should be generated when the bonds between a particle and its neighbours was broken. Initially, the damage growth in particle-particle bonds was developed independently of any other bonds in the neighbourhood of the i^{th} particle. Fig. 4 shows longitudinal stress history curve obtained at the back of the target plate (stress gauge location in Fig. 3.) from the experimental and simulation data. A plot of the simulation data without damage is also included to establish the tensile behaviour of the material and illustrate the spall effects. Note that in the simulation results, the stress data was plotted for the third particle into the PMMA to avoid noise in the simulation results originating from the material contact algorithm.

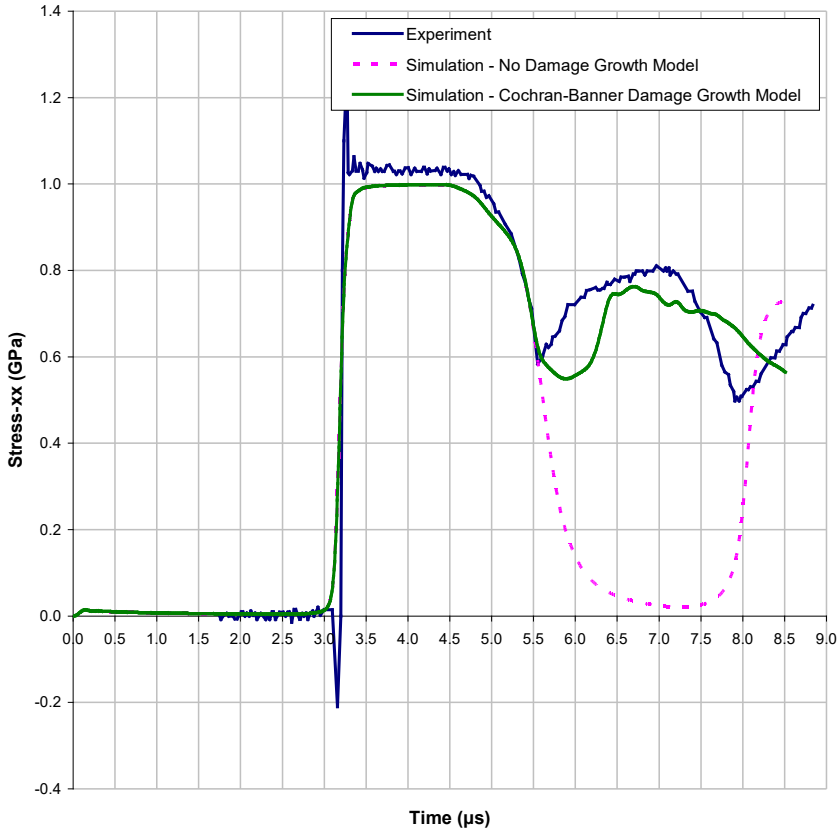

Fig. 4. Experimentally observed and numerically obtained stress traces at the back of the target plate; model with a single bond failure

It is clear from the results shown in Fig. 4 that the model predicted a failure of the particle bonds in the region of the expected spall plane, as a tensile reloading was obtained at the back of the target. However, the exact shape of the reload signal was not captured.

Following a discussion at the end of the previous section, local damage is likely to have an effect on the global behaviour of the material. This can be included in this model via a bond-break visibility criterion. Such a criterion is simple to implement in one-dimensional models, since any particle that is at least 2h from a free surface, will have an equal number of neighbours either side of it, as illustrated in Fig. 5. The criterion states that given that either of the bonds between the - particle and its first neighbour or the - particle and its second neighbour (on one side) have failed, then whichever bond is still active also fails. In the one-dimensional simulation case, a particle may have a maximum of four neighbours, two on each side. Consequently, if one bond fails, the other bond on that side also fails.

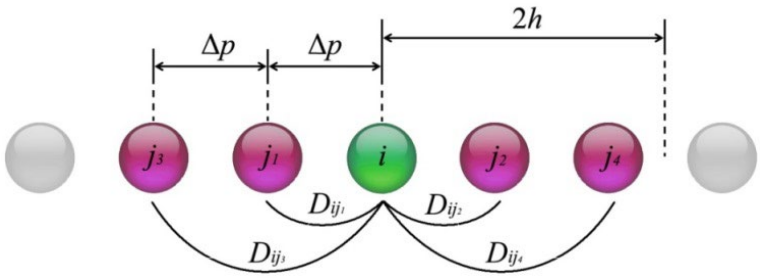

Fig. 5. Interaction of the ith particle with its neighbours in one dimensional problem

The effects of the activated bond break criterion are shown in Fig. 6, where three criteria for influence of multiple neighbours were considered:

1. if 1st neighbour failed then 2nd neighbour also failed;
2. if 2nd neighbour failed then 1st neighbour also failed;
3. If one failed, then the other bond also failed.

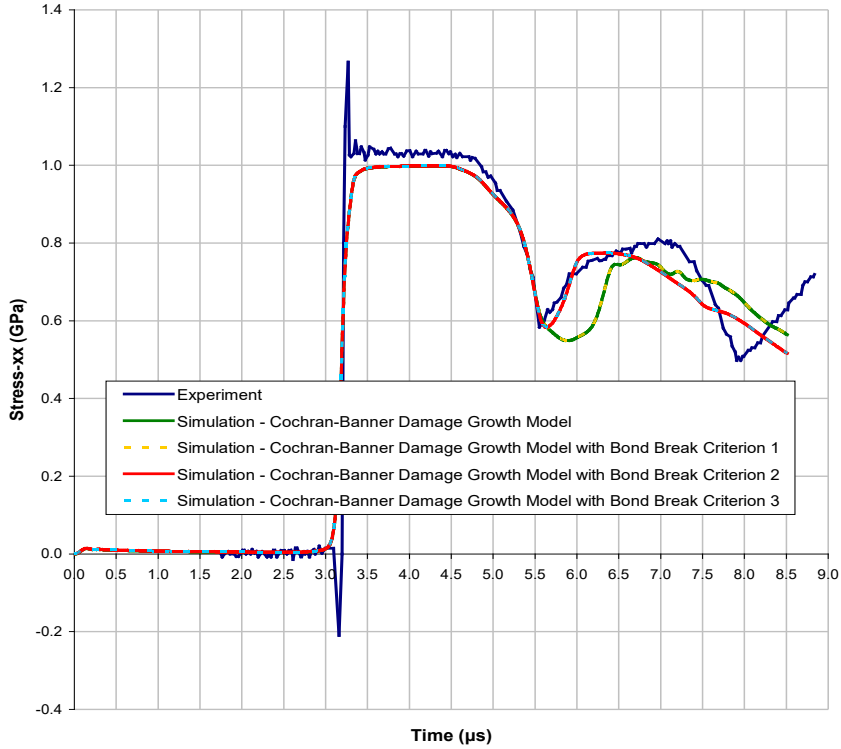

Fig. 6. Stress traces at the back of the target plate obtained with three criteria for interparticle interactions compared to the experimental data

Fig. 6 shows that the reload signal obtained with criterion two and three agree well with the experimental data. The remaining of the signal observed in this experiment is not a concern, since

the behaviour after the reload depends on the specific set-up of the experiment for which the data are not available. This set-up may not be represented in the simulation model and therefore it is unclear if a correlation should be observed.

Numerical validation was also performed with three-dimensional model of the plate impact tests shown in Fig. 7, with appropriate symmetry boundary conditions applied. The numerical results obtained with this model agree well with the experimental data as shown in Fig. 8.

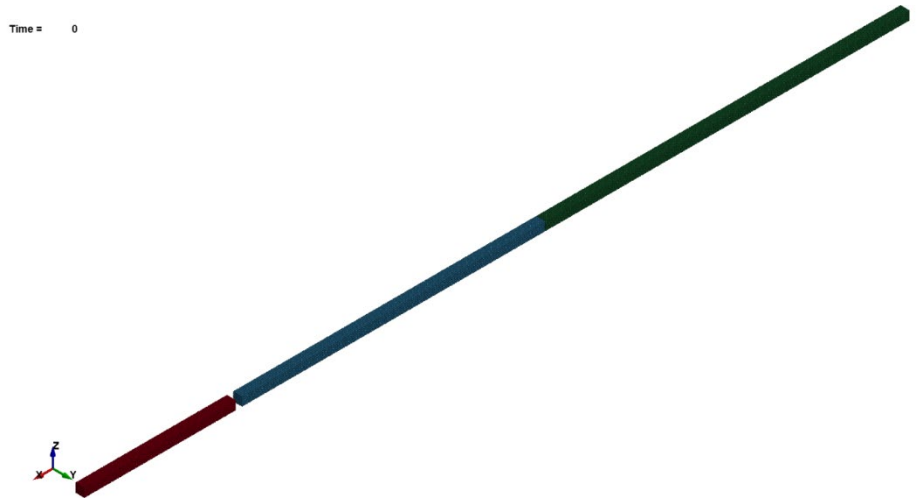

Fig. 7. 3D model of the plate impact test with appropriate symmetry conditions

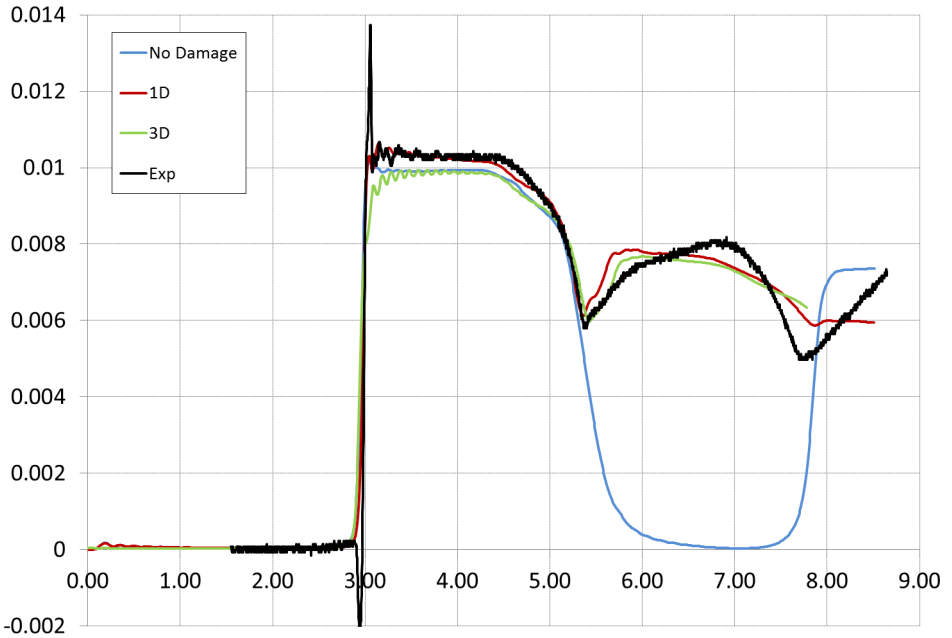

Fig. 8. Stress traces obtained at the back of the target plate with 3D model and compared to the experimental data

5.2 Tensile test with brittle failure model

A second test performed is a tensile test with a test sample geometry based on the ASTM3039 standard, used for characterisation of the tensile properties of polymer matrix composite materials. The initial configuration is shown in Fig. 9. The velocity is initialised as a linear velocity field distributed from zero at the fixed grip to the loading velocity (1.8m/s) at the moving grip, which largely eliminates the propagation of stress waves in the sample and is to a steady state test.

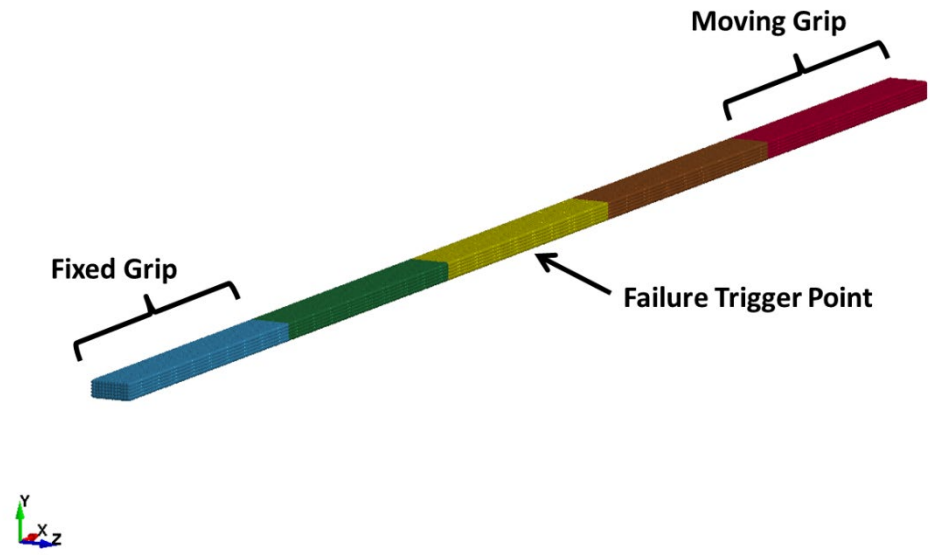

Fig. 9. Initial configuration for tensile test

The material used is linear elastic with brittle failure. The failure model sets the bond strength to zero once a critical stress has been reached.

Two symmetry planes of the tests, parallel to y and z plane in the middle of the sample, allowed for the reduction of the model size from ASTM3039 standard sample size to a quarter of the model. Consequently, thickness, width and the length of the model were respectively: 1mm, 5mm and 50mm + grips.

One particle at the middle of the sample length was assigned a failure stress of 95% of the nominal value, which triggers the failure at the centre of the sample, in the absence of any geometric or material property perturbations. Once failure has started, it propagates into a complete fracture and results in an unloading wave propagating through the sample, see Fig. 10.

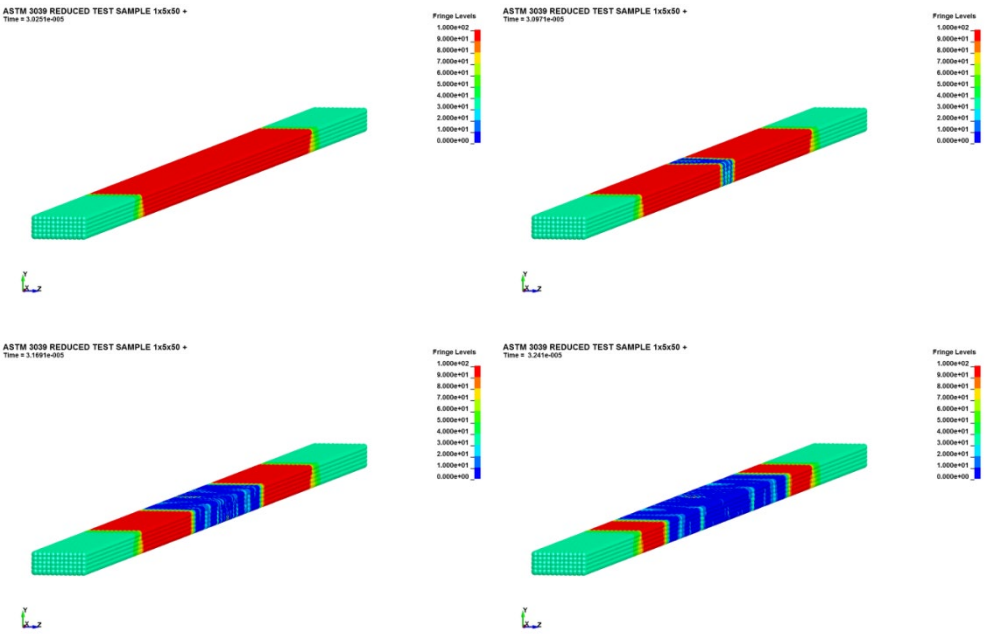

Fig. 10. Unloading wave travelling through the tensile test sample after a complete fracture developed in the centre

5.3 Hard projectile impact on a flat plate with brittle failure model

A third test performed is a ballistic impact on a flat plate. This test setup is inspired by the EASA CS-52 regulations for debris impact on fuel tank access covers. The test consisted of a flat plate and a cubical projectile with edge length of 9.5mm and a mass of 6.9g. The plate had a thickness of 3.175mm. Making use of the symmetry in the test configuration, a quarter model was used. The steel projectile was assigned elastic material properties, and the target material was defined as elastic with brittle failure. At failure, the particle-particle bond strength was set to zero. The initial state for an impact velocity of 240m/s is shown in Fig. 11. The evolution of failure and fragment generation is shown in Fig. 12. A number of large fragments developed as well as a series of smaller fragments and radial cracks. The modelling approach for treating damage at the inter-particle bonds is clearly reliable in this case.

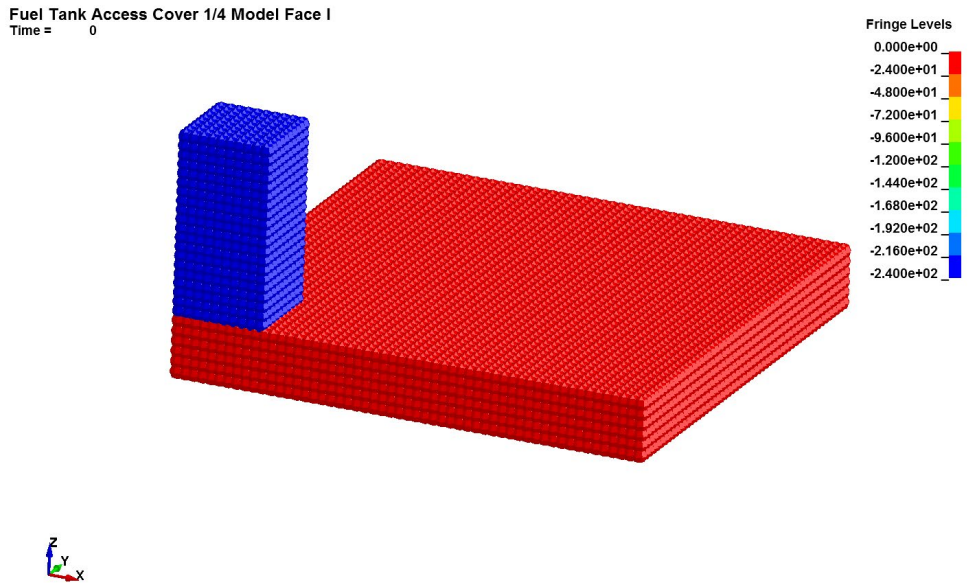

Fig. 11. Initial velocity field for cube impact model

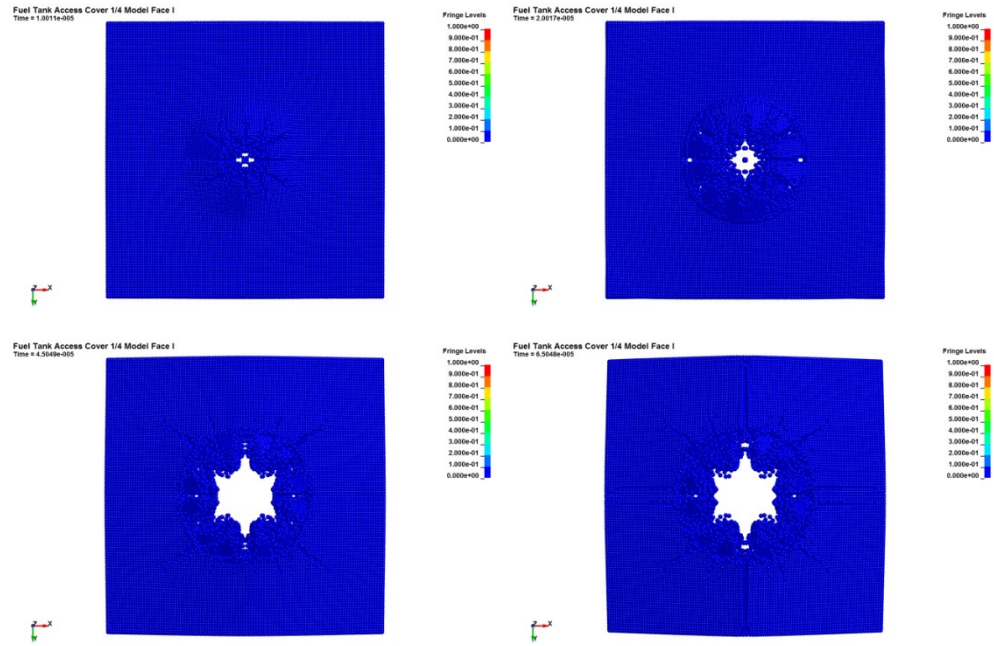

Fig. 12. Development of fragment and cracks in projectile impact on brittle plate

5.4 Spherical projectile impact on composite target plate

To demonstrate the use of an inter-particle damage model for composite materials, the approach described in Section 4.2.3 is applied to a hard projectile impact on a composite plate test. The test setup consists of composite panel with dimensions 200x200x6mm and spherical projectile, 12

mm in diameter, made of hardened steel with a nominal weight of 7 g. The composite panel consists of 23 unidirectional plies, which are 0.26mm thick, arranged in the stacking sequence [-45/0/+45/90]3S.

The model uses an elastic material for the projectile, and for the composite an elastic material with failure treated using the inter-particle damage model based on the Chang –Chang failure criteria described in Section 4.2.3. The model setup is shown in Fig. 13. The side view of the initial, intermediate state for the 138m/s impact is shown Fig. 14, with the front and back face deformations shown in Fig. 15. The projectile does not penetrate the sample, as observed in the test.

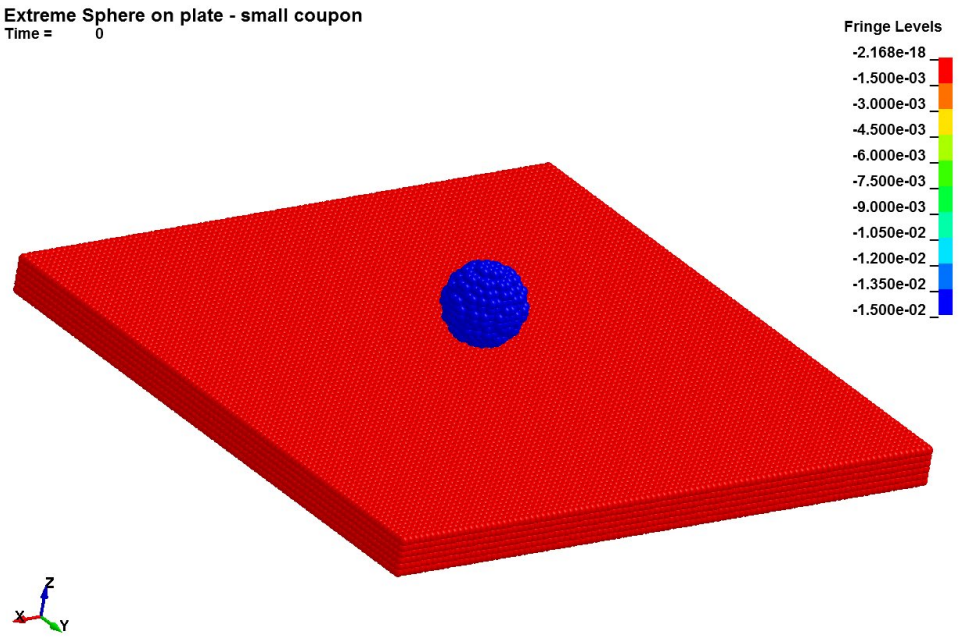

Fig. 13. SPH model of the hard projectile impact modelled with interaction area approach

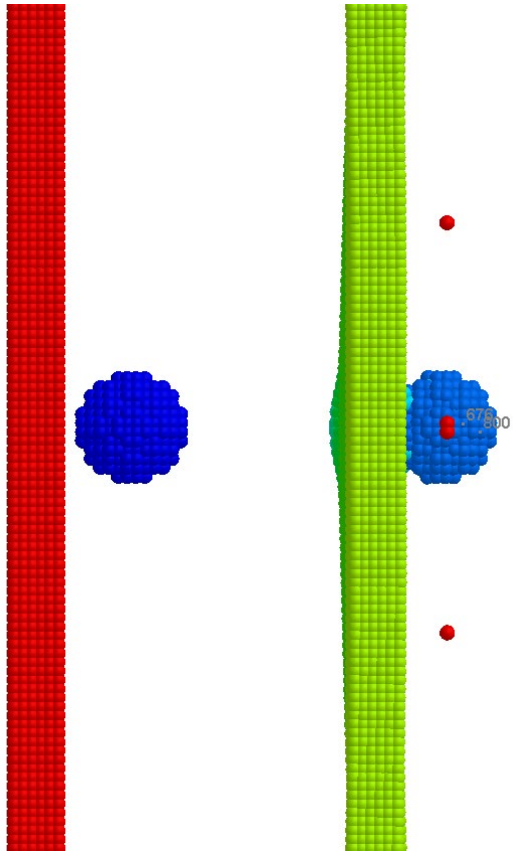

Fig. 14. Kinematics of deformation at maximum deflection in the simulation of the hard projectile impact at 138m/s

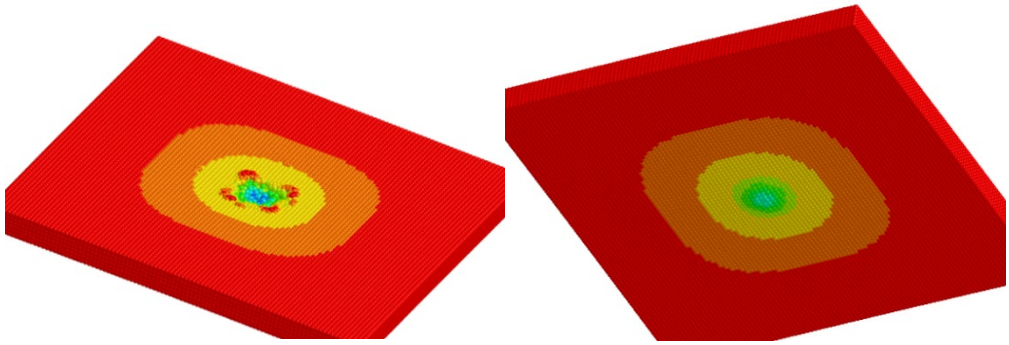

a) b)

Fig. 15. Damage distribution obtained at the front (a) and back face of composite panel (b)

6. Conclusions and future work

A damage modelling approach for high strain-rate loading has been developed based on the definition of the interaction area vector. The model is consistent with classical continuum damage

mechanics approach, but unlike the majority of other models, it does not require the use of an effective stress to incorporate the damage. The SPH momentum equation was rearranged in a way that it contained a particle-particle interaction area, so that damage or failure was defined to reduce this area until failure (critical damage), when the area was set to zero.

A number of different damage/failure initiation and growth criteria has been developed and tested:

1. Damage is initiated when the direct stress between particle pairs exceeds a spall criterion. A simplified Cochran-Banner damage growth model was implemented, to evolve the damage parameter, and coupled with a criterion for multiple neighbour particle bonds failure when one reached critical damage.

2. Immediate failure is initiated when Von Mises or Maximum stress criterion is met.

3. Orthotropic formulation with composite failure modes.

The model was used for simulation of three different tests with different failure modes:

1. Uniaxial plate impact tests were obtained with 1D and 3D models and they compared well with available experimental data.

2. ASTM 3039 tensile test;

3. Cube shaped projectile impact on a flat composite plate;

4. Sphere projectile impact on the composite target;

Future work on this development is integration of developed algorithms with the other damage models.

Acknowledgement: The project leading to this paper has received funding from the European Union's Horizon 2020 research and innovation programme under grant agreement No 636549.

References:

Belytschko T, Black T. (1999). Elastic crack growth in finite elements with minimal remeshing. *Int J Numer Methods Eng* 45:601–20. https://doi.org/https://doi.org/10.1002/(SICI)1097-0207(19990620)45:5<601:AID-NME598>3.0.CO;2-S.

Belytschko T, Guo Y, Kam Liu W, Ping Xiao S. (2020). A unified stability analysis of meshless particle methods. *Int J Numer Methods Eng* 2000; 48:1359–400. https://doi.org/https://doi.org/10.1002/1097-0207(20000730)48:9<1359:AID-NME829>3.0.CO;2-U.

Belytschko T, Tabbara M. (1996). Dynamic Fracture Using Element-Free Galerkin Methods. *Int J Numer Methods Eng* 39:923–38. https://doi.org/https://doi.org/10.1002/(SICI)1097-0207(19960330)39:6<923:AID-NME887>3.0.CO;2-W.

Chang F-K, Chang K-Y. (1987a). Post-Failure Analysis of Bolted Composite Joints in Tension or Shear-Out Mode Failure. *J Compos Mater* 21:809–33. https://doi.org/10.1177/002199838702100903.

Chang F-K, Chang K-Y. (1987b). A Progressive Damage Model for Laminated Composites Containing Stress Concentrations. *J Compos Mater* 21:834–55. https://doi.org/10.1177/002199838702100904.

Cochran S, Banner D. (1977). Spall studies in uranium. *J Appl Phys* 48:2729–37. https://doi.org/10.1063/1.324125.

Gingold RA, Monaghan JJ. (1977). Smoothed particle hydrodynamics: theory and application to non-spherical stars. *Mon Not R Astron Soc* 181:375–89. https://doi.org/10.1093/mnras/181.3.375.

Gravouil A, Moës N, Belytschko T. (2002). Non-planar 3D crack growth by the extended finite element and level sets—Part II: Level set update. *Int J Numer Methods Eng*, 53:2569–86. https://doi.org/https://doi.org/10.1002/nme.430.

Kachanov LM. (1958). Time of the rupture process under creep conditions, *Izy Akad. Nank SSR Otd Tech Nauk* 1958; 8:26–31.

Krysl P, Belytschko T. (1999). The Element Free Galerkin method for dynamic propagation of arbitrary 3-D cracks. *Int J Numer Methods Eng* 44:767–800. https://doi.org/https://doi.org/10.1002/(SICI)1097-0207(19990228)44:6<767:AID-NME524>3.0.CO;2-G.

Lemaitre J. (1985). A Continuous Damage Mechanics Model for Ductile Fracture. *J Eng Mater Technol* 107:83–9. https://doi.org/10.1115/1.3225775.

Libersky LD, Petschek AG. (1991). Smooth particle hydrodynamics with strength of materials. In: Trease HE, Fritts MF, Crowley WP, editors. *Advances in the Free-Lagrange Method Including Contributions on Adaptive Gridding and the Smooth Particle Hydrodynamics Method*, Berlin, Heidelberg: Springer Berlin Heidelberg;. 248–57.

Libersky LD, Petschek AG, Carney TC, Hipp JR, Allahdadi FA. (1993). High Strain Lagrangian Hydrodynamics: A Three-Dimensional SPH Code for Dynamic Material Response. *J Comput Phys* 109:67–75. https://doi.org/10.1006/JCPH.1993.1199.

Lucy L B. (1977). A numerical approach to the testing of the fission hypothesis. 82:1013–24. https://doi.org/10.1086/112164.

Malvern LE. (1969). *Introduction to the Mechanics of a Continuous Medium*. Prentice-Hall;

Mirkovic J. (2004). Modelling of Nonlinear Behaviour of Metallic Structure Components. PhD. Cranfield University.

Moës N, Dolbow J, Belytschko T. (1999). A finite element method for crack growth without remeshing. *Int J Numer Methods Eng* 46:131–50. https://doi.org/https://doi.org/10.1002/(SICI)1097-0207(19990910)46:1<131:AID-NME726>3.0.CO;2-J.

Moës N, Gravouil A, Belytschko T. (2002). Non-planar 3D crack growth by the extended finite element and level sets—Part I: Mechanical model. *Int J Numer Methods Eng* 53:2549–68. https://doi.org/https://doi.org/10.1002/nme.429.

Ortiz M, Pandolfi A. (1999). Finite-deformation irreversible cohesive elements for three-dimensional crack-propagation analysis. *Int J Numer Methods Eng* 44:1267–82. https://doi.org/https://doi.org/10.1002/(SICI)1097-0207(19990330)44:9<1267:AID-NME486>3.0.CO;2-7.

Pandolfi A, Krysl P, Ortiz M. (1999). Finite element simulation of ring expansion and fragmentation: The capturing of length and time scales through cohesive models of fracture. *Int J Fract* 95:279–97. https://doi.org/10.1023/A:1018672922734.

Rabczuk T, Belytschko T. (2004). Cracking particles: a simplified mesh free method for arbitrary evolving cracks. *Int J Numer Methods Eng* 61:2316–43. https://doi.org/https://doi.org/10.1002/nme.1151.

Rabczuk T, Belytschko T. (2007). A three-dimensional large deformation meshfree method for arbitrary evolving cracks. *Comput Methods Appl Mech Eng* 196:2777–99. https://doi.org/10.1016/J.CMA.2006.06.020.

Rabczuk T, Belytschko T, Xiao SP. (2004). Stable particle methods based on Lagrangian kernels. *Comput Methods Appl Mech Eng*, 193:1035–63. https://doi.org/10.1016/J.CMA.2003.12.005.

Reveles JR. (2007). *Development of a Total Lagrangian SPH code for the simulation of solids under impact loading*. PHD. Cranfield University.

Stolarska M, Chopp DL, Moës N, Belytschko T. (2001). Modelling crack growth by level sets in the extended finite element method. *Int J Numer Methods Eng* 51:943–60. https://doi.org/https://doi.org/10.1002/nme.201.

Standard Test Method for Tensile Properties of Polymer Matrix Composite Materials (2009) ;15.03.

Steinberg DJ. (1996).Equation of State and Strength Properties of Selected Materials. UCRL-MA-106439. Laurence Livermore National Laboratory.

Swegle JW, Attaway SW, Heinstein MW, Mello FJ, Hicks DL. (1994). An analysis of smoothed particle hydrodynamics. United States: https://doi.org/10.2172/10159839.

Swegle JW, Hicks DL, Attaway SW. (1995). Smoothed Particle Hydrodynamics Stability Analysis. *J Comput Phys*116:123–34. https://doi.org/10.1006/JCPH.1995.1010.

Swegle JW.(2000). *Conservation of Momentum and Tensile Instability in Particle Methods*. United States:. https://doi.org/10.2172/759439.

Ventura G, Xu JX, Belytschko T. (2002). A vector level set method and new discontinuity approximations for crack growth by EFG. *Int J Numer Methods Eng,* 54:923–44. https://doi.org/https://doi.org/10.1002/nme.471.

Vignjevic R, Reveles JR, Campbell J. (2006). SPH in a total lagrangian formalism. *CMES - Computer Modeling in Engineering and Sciences* 14.

Vignjevic R, Campbell J, Jaric J, Powell S. (2009). Derivation of SPH equations in a moving referential coordinate system. *Comput Methods Appl Mech Eng* 198:2403–11. https://doi.org/10.1016/J.CMA.2009.02.027.

Vignjevic R, DeVuyst T, Campbell J. (2021). The nonlocal, local and mixed forms of the SPH method. Comput Methods *Appl Mech Eng* 387:114164. https://doi.org/10.1016/J.CMA.2021.114164.

Vignjevic R, Campbell J, Libersky L. (2020). A treatment of zero-energy modes in the smoothed particle hydrodynamics method. *Comput Methods Appl Mech Eng* 184:67–85. https://doi.org/10.1016/S0045-7825(99)00441-7.

Xu XP, Needleman A. (1994). Numerical simulations of fast crack growth in brittle solids. *J Mech Phys Solids* 42:1397–434. https://doi.org/10.1016/0022-5096(94)90003-5.

Zhou F, Molinari JF. (2004). Dynamic crack propagation with cohesive elements: a methodology to address mesh dependency. *Int J Numer Methods Eng*; 59:1–24. https://doi.org/https://doi.org/10.1002/nme.857.